Korean J. Chem. Eng., 40(4), 999-1013 (2023)
DOI: 10.1007/s11814-022-1318-6

pISSN: 0256-1115
eISSN: 1975-7220

Highly efficient, durable and eco-friendly intumescent flame retardant for wool fabrics

Yan Gao* and Jinfeng Li,†**

*Centre of Analysis and Measurement, Jilin Institute of Chemical Technology, Jilin 132022, China
**School of Materials Science and Engineering, Jilin Institute of Chemical Technology, Jilin 132022, China
(*Received 1 July 2022 • Revised 11 September 2022 • Accepted 17 October 2022*)

Abstract−According to the requirements of flame retardant and environmental protection of wool fabrics, a phosphorus-nitrogen intumescent flame-retardant (IFR) system was constructed on the surface of wool fabrics based on dip-rolling-drying process with DEA serving as carbonizing agent, phosphorous acid and phosphoric acid used as acids, and urea serving as blowing agent. Ammonium N-ethoxy-n-methylene phosphonate-n-ethyl phosphate (ANPP) was designed and the treated wool fabrics with a weight gain (WG) of 27.4% presented highly flame retardancy and exhibited a high limiting oxygen index (LOI) of 37.8%; after 50 laundering cycles (LCs), LOI can still be remained at 30.5%. Self-extinguishing properties in the vertical combustion. The cone calorimeter (CONE) test verified that the peak heat release rate (PHRR) of the untreated wool fabrics declined to 82.2 from 251.7 kW/m^2 after ANPP treatment, and the total heat release (THR) was reduced to 4.4 from 37.9 MJ/m^2. In addition, the physical properties were maintained in the usable range. The flame-retardant mechanism analysis showed that the dense phosphorus-nitrogen char layer shaped effectively prevented the release of heat and spread of flammable volatile substances in the condensed phase. This study supplies novel ideas on devising and manufacturing of environmentally friendly treated wool fabrics with superior flame retardancy, durability, and high efficiency.

Keywords: Wool Fabrics, Flame Retardancy, High Efficiency, Durable

INTRODUCTION

Wool, protein fiber, has excellent properties, such as soft handling, firm texture, good elasticity, and warmth retention. It is often used for high-grade clothing and interior decoration products, and accessories. Although wool fabrics contain more flame retardant elements N (15-16 wt%), S (3-4 wt%), and high moisture retention (10-14 wt%) [1], its LOI can reach 23-24%, which has better natural flame retardancy compared with other fibers, such as, cotton, nylon, silk, and polyester. But it still cannot meet the requirements of some high-standard textiles. For example, there are high requirements for flame retardancy of textiles in medical and health protective clothing, military and police working clothing, and firefighters' firefighting clothing. Hence, how to realize the environment-friendly, high efficiency, durable, and flame retardancy of wool fabric is a key problem to be solved in textile fire safety research.

Cysteine is the most important amino acid among the 18 different amino acids of wool fabrics [2]. Cysteine containing disulfide bond is the reason for the low flammability of wool fabrics [3]. Nevertheless, it will still burn in the textiles-burning behavior-vertical method. The halogen flame retardant on textiles is a typical gas-phase flame-retardant mechanism. The hydrogen halide gas produced by thermal decomposition can capture a large number of active free radicals, $H^{\cdot}$, $O^{\cdot}$, and $OH^{\cdot}$, generated in the burning process of textiles, and generate halogen free radicals with low activity, so as to interrupt the combustion and give textiles outstanding flame retardancy [4]. However, halogen will harm biological thyroid and liver and has the risk of cancer. And thereby the EU and the United States have banned the production and use of halogen flame retardants [5]. Therefore, wool fabrics require further flame retardant finishing to improve their flame retardancy, durability, and environmental protection.

Among the new flame retardants developed successfully, inorganic flame retardants include metal oxides and hydroxides, inorganic silicon containing compounds, red phosphorus, and expandable graphite. Their use mode is mainly directly doped and filled into the matrix material, which can not only improve the fire resistance of the matrix material, but also inhibit the generation of smoke, be non-toxic, and non-corrosive [6]. Unfortunately, they effectively reduce flame spread. Although the heat release rate (HRR) of the treated samples has been found to be reduced, other important parameters, such as ignition time and THR, are relatively poor [7]. Very recently, flame retardants have been developing in the direction of sustainability, high efficiency, and low cost. Many natural polymers also contain phosphorus, nitrogen, and other elements. Phosphorus-nitrogen synergistic flame retardants refer to a kind of flame retardant containing phosphorus-nitrogen flame retardant elements in the system. Nitrogen containing compounds release noncombustible gases during thermal decomposition, and will expand the char layer in the presence of acid source (phosphorus containing compounds). The formation of a certain thickness of intumescent coatings can better isolate the heat spread and greatly enhance their flame retardancy. In addition, phosphorus-based flame retardants can form covalent bonds with wool fabrics and usually function in the condensed-phase stage [8-10]. Phosphorylation of wool fabrics keratin significantly improves char formation [11].

†To whom correspondence should be addressed.
E-mail: 2312329010@qq.com

The study on the flame retardant finishing has presented that it has achieved certain results in the flame retardant performance of wool fabrics. Cheng et al. designed polyelectrolyte complex (PEC) flame retardant with phytic acid (PA) and chitosan as raw materials for flame retardant finishing of wool fabrics. The flame retardant performance of the treated wool fabrics was significantly improved. However, five depositions reduced from B2 classification to B1 classification, and the LOI decreased from 34 to 28% after 10 LCs [12]. Cheng et al. also developed the PA/TiO_2/1, 2, 3, 4-butanetetracarboxylic acid (BTCA) system giving wool fabrics outstanding durable flame retardancy. The LOI enhanced to 34.4% with a WG of 13.0%, and the char length decreased to 9.8 cm. After 5 LCs, the LOI still maintained 30.2% and char length was to 10.3 cm, giving the wool fabrics excellent flame retardancy and durability [13]. Mathur et al. studied the flame retardant effect of P-S compound, looking at the synergistic effect on wool fabric. When the addition amount was 16.65%, the LOI of treated wool fabrics was improved from 25.0% to 35.8%, and the char length was reduced from complete burning to 3.3 cm. While the PHRR decreased by 44.57% and the THR decreased by 30.30%, indicating that the treated wool fabrics plays a flame retardant effect in the condensed phase. After 30 LCs, the LOI declined to 25.3% and char length increased to 7.0 cm [14]. Zhou et al. synthesized cyclotriphosphazene keratin (CCTPK) flame retardant from hexachlorocyclotriphosphazene (HCCTP) and FK, and prepared CCTPK blended viscose fiber by wet spinning technology. LOI of flame retardant viscose fiber containing 10% (mass fraction) CCTPK flame retardant reached 28.6%. CCTPK flame retardant can significantly improve the flame retardancy of viscose fiber, which decreased to 27.5% after 30 LCs, but the durability needs to be improved [15]. The above research progress prompted us to apply IFR system to develop durable flame retardant wool fabrics.

Relevant studies show that flame retardants containing both phosphorous and nitrogen are more efficient than those containing only phosphorous or nitrogen [16-18]. In the present work, wool fabrics made by finishing with dip-rolling-drying process were assessed, and are expected to prepare durable flame retardant wool fabric. The effect of WG on the wool fabrics was evaluated. The flame retardancy, durability, and thermal stability of the treated wool fabrics were discussed by LOI, vertical combustion, CONE, and thermogravimetry (TG) test. Scanning electron microscopy-energy dispersive spectroscopy (SEM-EDS) was applied to analyze the surface morphology and element composition of the wool fabrics and the char residue. Finally, the flame retardant mechanism of wool fabrics char residue was analyzed by Raman and X-ray photoelectron spectrometry (XPS).

EXPERIMENTAL SECTION

1. Materials

100% woven wool fabrics (130 g/m^2) were acquired from Jilin city, China. Before surface modification, they were rinsed to remove impurities on the surface, and dried in an oven for standby. Formaldehyde solution (37%) was purchased from Chongqing Chuandong Chemical Reagent Co., Ltd. (Chongqin, China). Phosphorous acid (85%) was provided by Aladdin reagent (Shanghai) Co., Ltd. (Shanghai, China). DEA, phosphoric acid, urea, ethanol, and dicyandiamide were purchased from Chengdu Kelong Chemical Reagent Co., Ltd. (Chengdu, China). All purchased reagents could be used directly without further purification.

2. Synthesis and Characterization of ANPP

At room temperature, Diethanolamine (0.6 mol), HCHO (0.6 mol), and distilled water were added to a four-mouthed flask with 200.00 mL of 5% $KMnO_4$ aqueous solution to absorb the formaldehyde released by the system. When the temperature of the system reached 45 °C, 0.6 mol phosphorous acid was poured into the solution and a pale yellow solution was acquired (**a**, Intermediate I). After which, the mixture was reacted at 95 °C for 100 min. Then, the solution was poured into the beaker. 0.6 mol phosphoric acid was poured slowly into the beaker and heated at 140 °C for 4.5 h to obtain a viscous yellow liquid (**b**, Intermediate II). 1.2 mol urea was added to the above mixture under mechanical stirring and heated at 150 °C for 1 h. After the reaction, a crude yellow solid (**c**, ANPP) was produced, which was purified three times with absolute ethanol and dried in an oven with a yield of 77.3%. Scheme 1 describes the reaction route of ANPP, and digital images of (a),

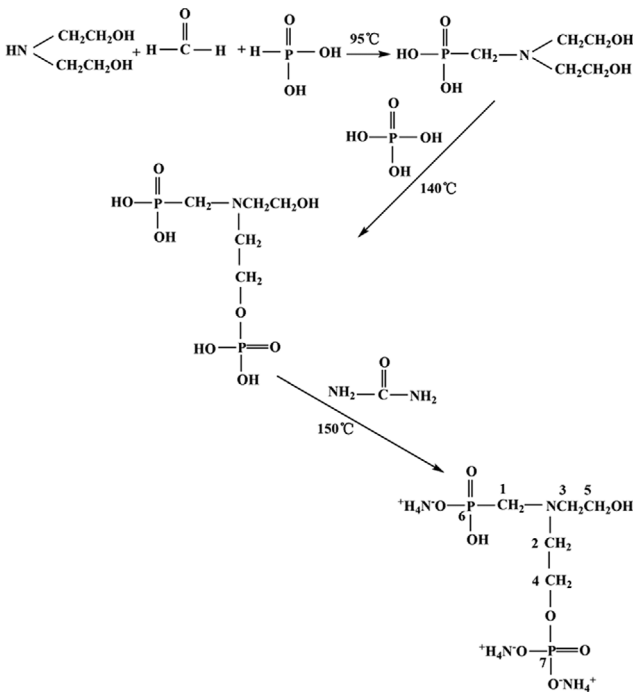

Scheme 1. Synthesis reactions of ANPP.

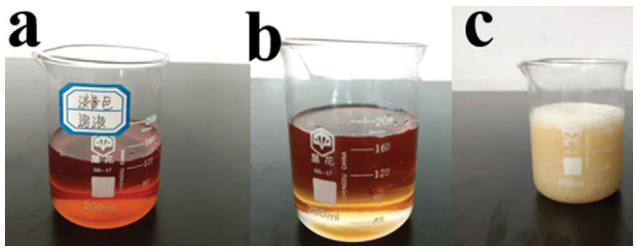

Fig. 1. Digital photos of (a, Intermediate I), (b, Intermediate II), and (c, ANPP).

(b), and ANPP (c) are shown in Fig. 1.

NMR data of ANPP is as follows:

^{1}H NMR (D_2O, 600 MHz; δ (ppm)): 2.13 (s, 1CH_2, H_1), 2.94 (m, 1CH_2, H_2), 2.68 (m, 1CH_2, H_3), 3.99 (m, 1CH_2, H_4), and 3.24 (m, 1CH_2, H_5).

^{13}C NMR (D_2O, δ (ppm)): 48.05 (1C, C_1), 54.35 (1C, C_2), 59.56 (1C, C_3), 67.28 (1C, C_4), and 57.37 (1C, C_5).

^{31}P NMR (D_2O, δ (ppm)): 2.54 (P_6), and 0.33 (P_7).

The NMR results are consistent with the chemical structure of the target product ANPP.

3. ANPP Treatment of Wool Fabrics

ANPP was dissolved in water to prepare flame retardant solutions with aspecific concentration, clean wool fabrics were immersed in these solutions, and dicyandiamide with mass fraction of 5% was added as catalyst. The reaction was shaken on a constant temperature oscillator at 70 °C for 30 min. The wool fabrics were extruded by a vertical small rolling car. Two dippings and two rollings ensured that the liquid carrying rate of wool fabrics impregnated with ANPP solution reached 80%, and then the wool fabric was pre-dried on an 80 °C continuous heat setting dryer for 10 min, and baked and cured 160 °C for 3 min. After removal, the surface was washed with flowing water and dried in an oven at 60 °C.

The WG% is determined by Eq. (1):

$$w = \frac{m_1 - m_0}{m_0} \times 100\% \quad (1)$$

In which, m_0 is the weight of untreated wool fabrics, g; and m_1 is the weight of treated wool fabrics, g.

4. Characterization

^{1}H, ^{13}C, and ^{31}P NMR (nuclear magnetic resonance) of ANPP was characterized on a Bruker Avance NEO 600 spectrometer using D_2O as the solvent. The Fourier transform infrared (FT-IR) spectra were recorded by an FT–IR spectrometer in the 4,000-500 cm^{-1} range at a resolution of 2.0 cm^{-1} to analyze the ANPP, untreated and treated wool fabrics.

The whiteness and yellowness of the untreated and treated wool fabrics were conducted on a whiteness colorimeter in accordance with GB/T 8424.2-2001. The fabric was folded in half three times and put into the tester for test. Each sample was measured five times and the average value was taken.

The tensile strength of the untreated and treated wool fabrics was determined in accordance with GB/T 3917.3-2009 standard on a micro controlled electronic universal testing machine. The fabric was cut into 50 mm in warp and weft directions×150 mm size, the test was repeated five times for each sample with tensile rate of 20 mm/min.

The strip sample was placed flat on the measuring plane of the instrument following the standard of GB/T 18318.1-2009 on a M507 fabric stiffness tester, and then moved forward slowly to make one end of the sample gradually separate from the plane support and form a cantilever. Under the gravity of the sample itself, when one end of the sample bent down to contact with the 41.5 inclined plane, the extension length was measure and the bending length and bending stiffness of the fabric was calculated.

The formaldehyde emission of the treated wool fabrics was evaluated by GB/T 2912.1-2009 (water extraction) by a textile formaldehyde tester. When the tested result was less than 20 ppm, the free formaldehyde emission of the wool fabrics was "not detected". We took 1 g (accurate to 10 mg) from the chopped sample, put it into a 250 mL iodine measuring bottle with a stopper, add 100 mL of water, covered the cover tightly, kept the constant temperature water bath at 40±2 °C for 60±5 °C, and shook the bottle every 5 min. Then cooled and filtered, took 5 mL of filter solution, added 5 mL of prepared hexamine acetone solution, shook it well, and kept it at constant temperature (40±2) °C for 30±5 min. After taking it out, placed it at room temperature for (30±5) min, and measured the absorbance at 412 nm.

The crystal structure information of untreated and treated wool fabrics was analyzed by X-ray powder diffraction (XRD). The test ray was Kα of Cu, the radiation ray, tube voltage and tube current were 36 kV and 20 mA, respectively, and the scanning step was 0.01°. The position, intensity and width of diffraction peak were recorded.

The surface morphology of the samples was observed by SEM at an accelerating voltage of 20 kV. EDS was utilized to detect the element content on the sample surface.

The LOI refers to the national standard ASTM d2863-2000 and is tested under standard conditions. The sample to be tested needs to be dried in an oven at 80 °C for 4 h, and the gas in the oxygen cylinder and nitrogen cylinder is not less than 5 MPa. The test data were recorded and printed. Under the standard experimental conditions, when oxygen and nitrogen were mixed, the lowest oxygen concentration of the tested sample during combustion was the limiting oxygen index. Through the limiting oxygen index test, the flame retardant effect of the flame retardant can be evaluated intuitively.

The washing method can test the water washability of flame-retardant wool fabrics. The standard washing conditions refer to AATCC 61-2006 standard. Put the sample into the stainless steel washing tank, put the iron ball, pour in the standard detergent, set the washing temperature at 40 °C, the rotating speed at 40 R/min, and each washing time is 30 min. One washing was equivalent to five washings in a family. After washing, the sample was taken out, rinsed and dried with clean water for standby.

The combustion performance of the wool fabrics before and after ANPP treatment was surveyed in the vertical state based on the standard of GB/T 5455-2014. The samples with dimensions of 300×90 mm^2 were suspended vertically on the burner for 19 mm and exposed to a flame (20 mm) for 12 s. Once the ignition source was removed, the corresponding data in the vertical direction were recorded.

The CONE test was applied to assess the combustion process of samples, which is 100×100×40 mm^3 under a heat flux of 50 kW/m^2 according to the ISO 5660-1 standard.

The thermal stability and oxidation resistance of the samples in nitrogen and air atmosphere were measured by thermogravimetric analyzer. After the sample was cut and crushed, we weighed about 5-6 mg of the treated sample and put it into a small crucible. According to the heating rate of 10 °C/min and the gas flow value of 30 mL/min, the thermal stability and oxidation resistance of the sample in the temperature range of 40-600 °C were explored.

The heat capacity of the wool fabrics before and after ANPP treatment in nitrogen atmosphere was estimated on a DSC from 40 to 350 °C at a rate of 10 °C/min.

Raman spectra is an effective means to reflect the graphitization degree of residual carbon. Raman spectra of the samples were performed with a laser Raman spectrometer with a range of 500-2,000 cm^{-1}, the excitation wavelength was 532.17 nm and integration time was 10 s.

XPS was used to explore the composition and content of chemical elements for the wool samples. The tube voltage was 36 kV, the tube current was 20 mA, and the scanning step was 0.01°. The performance of radiation ray was evaluated, and the relevant information of diffraction peak position, width, intensity and content was obtained.

RESULTS AND DISCUSSION

1. Structural Characterization of ANPP

Fourier transform infrared spectroscopy can qualitatively analyze different chemical bonds or functional groups in organic molecules. As shown in Fig. 2, the peaks located at 3,400 and 2,950 cm^{-1} demonstrate absorption of -OH bonds and the stretching of C-H bonds from the CH_2, respectively [19]. The new strong absorption peak at the wave number of 1,250 cm^{-1} was ascribed to the stretching vibration of P=O, and the absorption peak at 1,000 cm^{-1} corresponds to the P-O-C bonds. The peak at 870 cm^{-1} can be attributed to the P-OH stretching vibration, respectively [20,21]. Phosphorus and P-O-C, P=O functional groups were introduced into the wool fabrics before and after flame retardant finishing, which showed that the flame retardant molecules were successfully grafted onto the wool fiber.

2. Physical Properties Analysis

Physical properties are very important for the practical application of wool fabrics, and the detailed data are summarized in Table 1, the wool fabric treated with 10%, 20%, 30%, and 40% ANPP solutions were 9.1%, 18.7%, 27.4%, and 35.7%, respectively. The whiteness of wool fabric is adversely affected by ANPP deposition, which is caused by the inherent yellow and high temperature finishing of ANPP solution [22]. However, the introduction of ANPP can bridge the molecular chain of wool fiber, inhibit the slip effect of molecular chain, and help to improve the tensile strength of wool fabric. At the same time, the bending length and bending stiffness of the treated wool fabric increased slightly with the increase of WG, which had an adverse effect on the softness of the wool fabric.

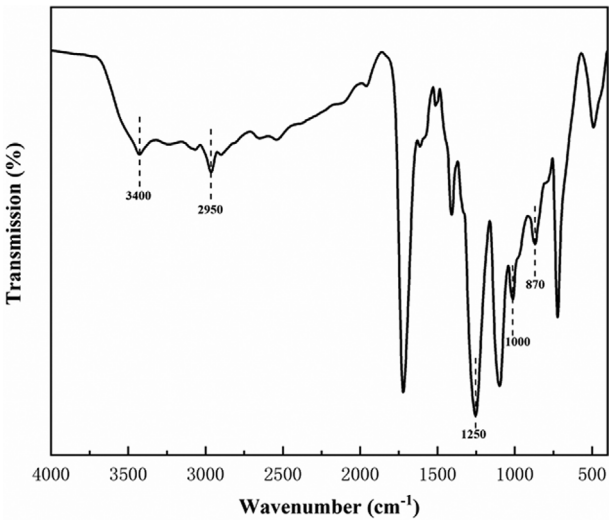

Fig. 2. The FT-IR spectra of ANPP.

The bending length of the wool treated with 27.4% WG increased by 20.3%, and the whiteness decreased by 11.9%. No formaldehyde release was detected (Formaldehyde content <20 ppm). This indicated that the phosphorus-nitrogen coating had almost no effect on the physical properties of wool fabrics and the physical properties remained within 70%, However, the whiteness of the treated wool fabrics decreased, and the bending length and flexural rigidity increased obviously with a WG of 33.7%.

3. FT-IR and XRD Analysis

FT-IR can qualitatively analyze different chemical bonds or functional groups in organic molecules. Fig. 3(a) shows the infrared spectra of wool fabrics before and after finishing with a WG of 27.4%, respectively. For wool fabric, the absorption peaks at wave numbers 3,416 and 2,917 cm^{-1} are caused by the stretching vibration of O-H and C-H, respectively [23]. There is a new strong absorption peak at the wave number of 1,247 cm^{-1}, which is caused by the stretching vibration of P=O. There is a weak P-OH stretching vibration absorption peak at 916 cm^{-1}; In addition, the P-O-C and stretching vibration was enhanced at 1,030 cm^{-1} absorption peak [24,25], which indicates that flame retardant molecules have been successfully introduced into the wool fiber. The absorption peak at 1,625 cm^{-1} is caused by the stretching vibration of C=O, which is because the glycosidic bond of cellulose is oxidized to C=O under high temperature and acidic environment [26]. P-O-C and P=O functional groups are introduced into the wool fabric before and after ANPP finishing, which shows that the flame retar-

Table 1. Physical properties values of the wool fabrics before and after ANPP finishing

A specific concentration (%)	WG (%)	Whiteness index (%)	Tensile strength (N)	Bending length (mm)	Flexural rigidity (mN cm)	Formaldehyde content (ppm)
0	-	84.3±0.2	255.3±8.2	15.3±0.2	0.846±0.052	-
Treated with 10%	9.1±0.1	79.2±0.1	283.4±5.7	16.9±0.4	0.983±0.064	6.4±0.08
Treated with 20%	18.7±0.3	76.5±0.3	286.8±4.3	17.3±0.3	1.244±0.072	12.5±0.17
Treated with 30%	27.4±0.2	74.3±0.2	290.4±3.1	18.4±0.5	1.472±0.068	18.2±0.12
Treated with 40%	35.7±0.3	70.2±0.1	287.6±3.8	21.0±0.7	1.621±0.135	26.1±0.22

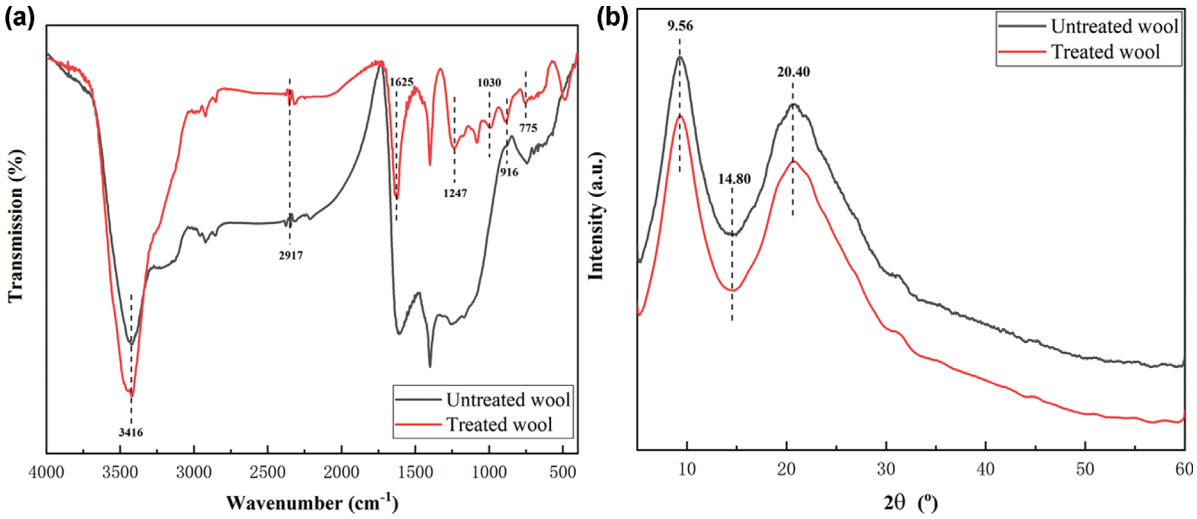

Fig. 3. (a) FT-IR and (b) normalized XRD curves of the untreated and treated wool fabrics.

dant molecules are successfully grafted onto the wool fabric.

The wool fabric before and after finishing with a WG of 27.4% was tested by X-ray powder diffraction analysis, and the test spectrum is presented in Fig. 3(b). It can be seen that the peak positions and peak types of the two samples are very similar, but the intensity of the three prominent diffraction peaks of the flame-retardant treated wool fabric is slightly weaker than that of the untreated wool fabric. During the process of soaking the ANPP finishing solution of the wool fabric, dicyandiamide and ammonium glyceryl triphosphate infiltrated into the amorphous region of the wool fiber, and these small molecular substances were grafted into this region in the subsequent high-temperature grafting reaction. Thus, the proportion of crystalline zone of wool fabric grafted with certain quality flame retardant decreased, resulting in the decrease of diffraction peak intensity. Comparing the two diffraction patterns, it can be found that the two sample fabrics are in 2θ=the two diffraction peaks of 9.56° belong to the (001) crystal plane, 2θ=the two diffraction peak of 14.80° is attributed to the (1-10) crystal plane [27], 2θ=the diffraction peak of 20.40° is attributed to the (002) crystal plane, which is consistent with the crystal plane characteristics of type I cellulose, which shows that the mild flame retardant finishing process has not greatly affected the original main structure of the fiber.

4. Surface Morphology and Element Content Analysis

The microstructure and element content of wool fabrics before and after ANPP flame retardant modification were observed by SEM-Mapping-EDS. Fig. 4 depicts SEM images for the untreated and treated wool with 27.4% WG at different magnifications. Fig. 4 (a_0, a_1, and a_2) clearly displays typical scaly structure of wool fibers, and has smooth surface, complete structure and clear outline. After the ANPP finishing, the scaly structure of wool fibers becomes fuzzy, some granular substances adhere to the surface of wool fiber, which is attributed to the adsorption of ANPP. It is interesting that a layer of film was tightly attached to the surface of the treated wool (Fig. 4b_0, b_1, and b_2), reflecting that the wool fibers have been successfully modified by the ANPP. In addition, the element distribution maps of the surface for the untreated and treated wool are presented in Fig. 4; notice that all elements are evenly distributed. At the same time, the distribution of these elements presents a clear fiber shape similar to the original wool fiber. And the detailed element contents are listed in EDS images. The untreated wool fabrics consist of C, O, and N elements. For the treated wool fabrics, P element was detected and the content of N element increased significantly to 20.14 from 14.84% of the untreated wool fabrics. Suggesting that the phosphorus-nitrogen coating was evenly deposited on the surface of the wool fabrics.

5. LOI Analysis

LOI, an index used to evaluate the combustion performance of materials, refers to the lowest O_2 concentration required for the materials in the O_2/N_2 mixture to maintain the combustion state

Table 2. The related LOI value of the wool fabrics before and after ANPP finishing

Sample	Untreated wool	Treated wool							
-	LOI (%)	WG (%)	LOI (%)	WG (%)	LOI (%)	WG (%)	LOI (%)	WG (%)	LOI (%)
0 LCs	24.0±0.3	9.1	28.9±0.07	18.7	31.6±0.05	27.4	37.8±0.12	35.7	38.2±0.05
10 LCs	-	8.3	28.1±0.08	15.7	30.4±0.13	24.3	35.7±0.08	31.2	36.9±0.09
20 LCs	-	7.5	27.5±0.06	12.5	29.9±0.09	22.6	34.2±0.14	29.4	35.5±0.13
30 LCs	-	6.2	26.7±0.07	11.9	28.3±0.16	21.8	32.8±0.09	28.6	34.2±0.15
40 LCs	-	5.9	26.0±0.14	10.7	27.5±0.13	20.2	31.6±0.10	27.1	33.9±0.09
50 LCs	-	5.0	25.4±0.09	9.6	26.6±0.07	19.3	30.5±0.07	26.4	33.1±0.14

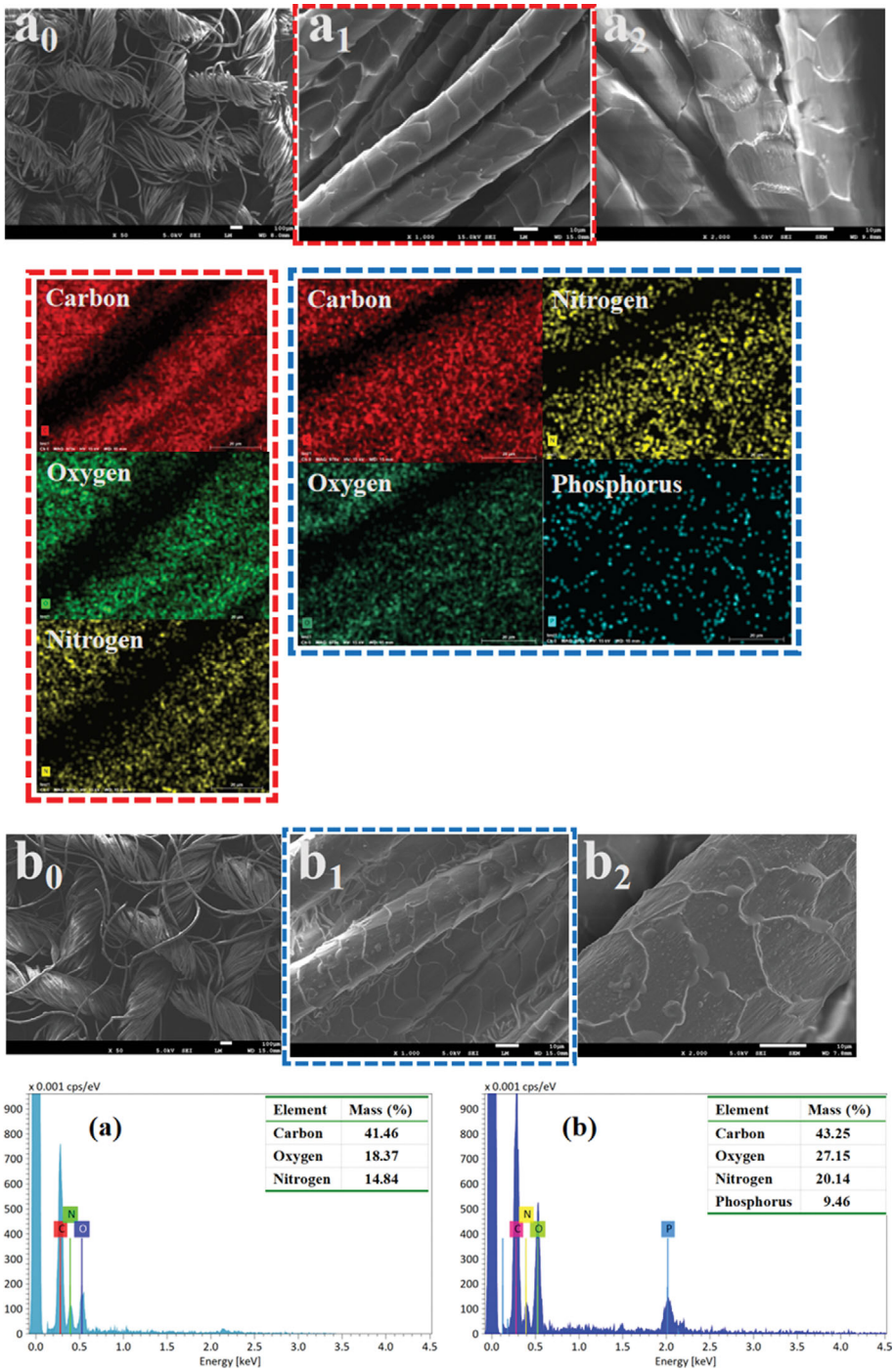

Fig. 4. a_0, a_1, a_2 SEM images for the untreated and b_0, b_1, b_2 treated wool fabrics; (a) EDS images for the untreated and (b) treated wool fabrics.

under the specified test conditions [28]. To obtain the durability of wool fabrics, the LOI and WG values of the untreated and treated wool fabrics data are listed in Table 2; the wool fabrics treated with 9.1%, 18.7%, 27.4%, and 35.7% WG had LOI values reaching 28.9%, 31.6%, 37.8%, and 38.2%, respectively. With the increase of LCs, the WG and LOI values of the treated wool fabrics reveal a downward trend. After 50 LCs, the WG values of the treated wool fabrics decreased to 5.0%, 9.6%, 19.3%, and 26.4%, respectively. And the LOI values were also decreased to 25.4%, 26.6%, 30.5%, and 33.1%, respectively. As can be observed, wool fabrics with 27.4% WG or more can be regarded as durable wool fabrics, which are higher than the LOI values of the international flame retardant standard (28.0%) [29]. It is responsible for the close combination of phosphorus and nitrogen components with wool fabrics through covalent bonds. Thus, in the washing process, the flame retardant components are not easy to be washed away, so as to ensure the durability of wool fabrics. Note that when the weight gain of treated wool is higher than 27.4%, LOI does not improve significantly, in-

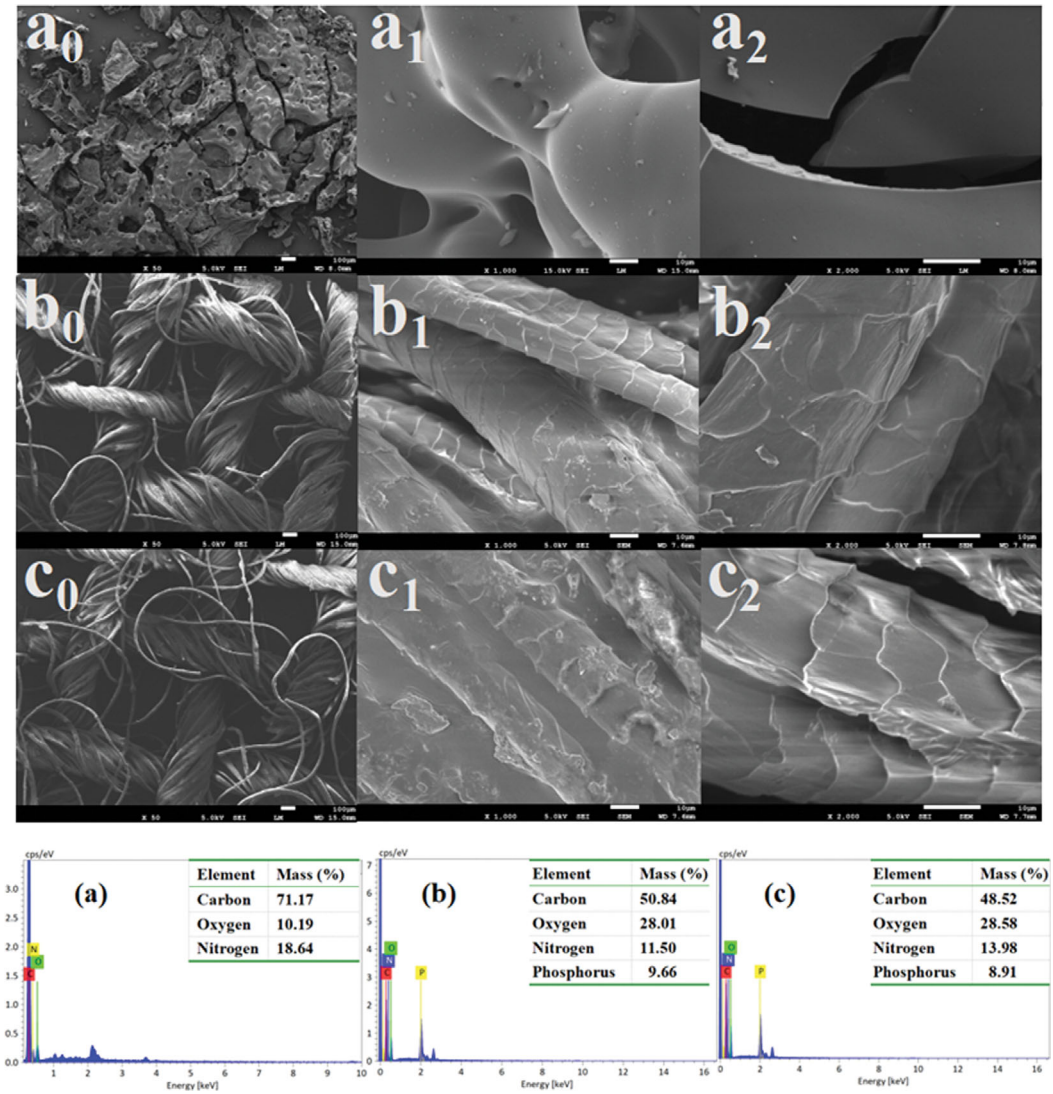

Fig. 5. SEM of the a_1, a_2, a_3 untreated, b_1, b_2, b_3 treated wool fabrics and c_1, c_2, c_3 after 50 LCs, EDS of (a) untreated, (b) treated wool fabrics and (c) after 50 LCs for the char residue after LOI test.

dicating that the effective P-N coating has reached saturation on wool fabrics.

The char residue of the samples after LOI test was evaluated by SEM-EDS. As displayed in Fig. 5, the char residue for the untreated (a_0, a_1, a_2), treated with 27.4 WG% before (b_0, b_1, b_2) and after 50 LCs (c_0, c_1, c_2) wool fabrics is presented in Fig. 5. It is clearly seen that the loose and non-fibrous char residue of the untreated wool fabrics have poor char forming ability. In comparison, the char residue of treated wool fabrics still maintains the morphological structure of warp and weft and has a large number of fibrous substances, and the surface is covered with a complete and dense char layer. The dense char layer isolates heat and oxygen during the combustion of wool fabrics and effectively seals various volatile products, which are released by the decomposition of wool fabric; when it comes into contact with oxygen and heat, it may cause further combustion degradation. What is more, the EDS results are obvious as shown in Fig. 5(a), (b), and (c) and the new element phosphorus is detected in the char residue for the treated wool fabrics. The phosphoric acid or polyphosphate generated during heating migrates to the surface of wool fiber, catalyzes the dehydration and carbonization of wool cellulose and reduces the molecular chain fracture. While, the ANPP particles on the fiber decompose in advance when heated, forming a thermally stable barrier, forming a graphitized carbon layer, preventing the spread of flame, and making the wool fabric have excellent flame retardant performance. This indicates that the treated wool fabric is accompanied by condensed phase flame retardant mechanism during heating. In the process of washing, the P content in the treated wool fabrics presents a downward trend similar to LOI. It can be speculated that the decrease of flame retardant effect of treated wool fabric is due to the decrease of P content. After 50 LCs, the P content remained at a high level, and the LOI remained at 30.5%, indicating that the wool fabric has excellent flame retardancy and durability.

6. Vertical Burning Analysis

Vertical burning results of the untreated (Fig. 6a) and wool fabrics treated with 9.1%, 18.7%, 27.4%, and 35.7% WG before (Fig.

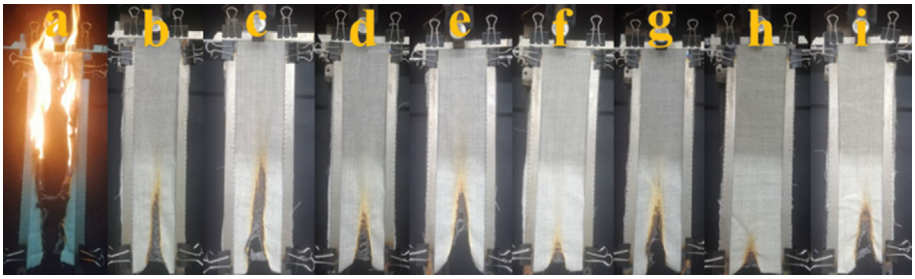

Fig. 6. Vertical burning tests for the a untreated and b, d, f, h wool fabrics treated with 9.1, 18.7, 27.4, and 35.7% WG and c, e, g, i after 50 LCs.

Table 3. Correlation values of the vertical burning results for the wool fabrics before and after ANPP finishing

WG (%)	LCs	Vertical burning test			
		t_1 (s)	t_2 (s)	Char length (cm)	UL-94
0	-	14±0.5	13±0.7	Burnt completely	V-2
9.1	0	10±0.1	11±0.2	7.9±0.15	V-1
	50	12±0.2	12±0.1	11.4±0.43	
18.7	0	3±0.12	4±0.15	6.1±0.12	V-0
	50	5±0.14	7±0.19	9.6±0.36	
27.4	0	0	0	3.1±0.18	V-0
	50	0	0	7.1±0.21	
35.7	0	0	0	2.4±0.09	V-0
	50	0	0	6.3±0.16	

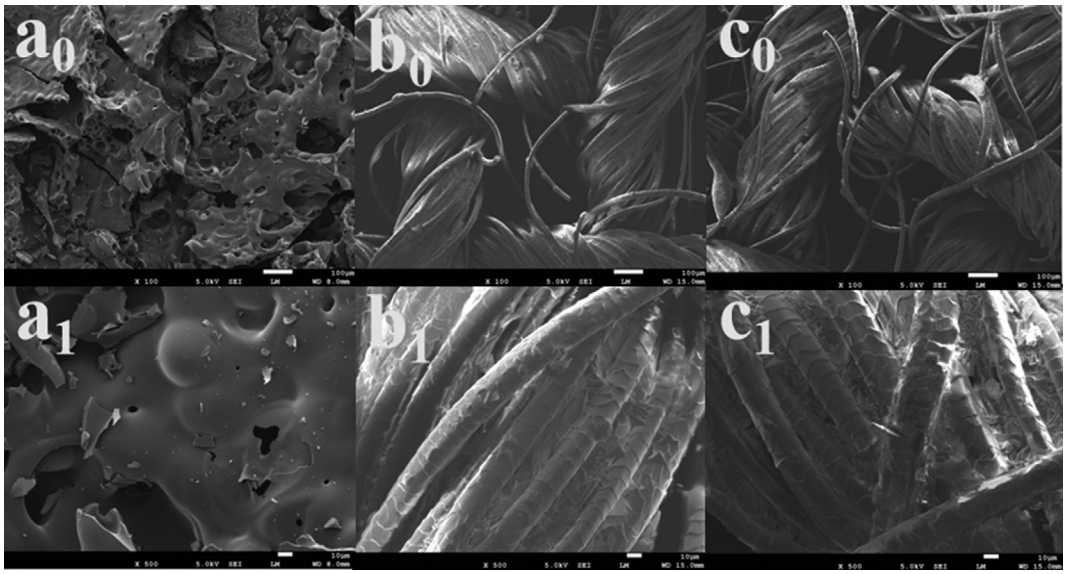

Fig. 7. Vertical burning test char residue of SEM for the a_0, a_1 untreated, b_0, b_1 treated wool fabrics and c_0, c_1 after 50 LCs.

6b, d, f, h) and after 50 LCs (Fig. 6c, e, g, i) are presented and the crucial data are listed in Table 3. In the burning area, it may be noticed that the untreated wool curls up during combustion to produce open fire and a large amount of smoke that burns quickly and completely. The after-flame time (t_1) and after-grow time (t_2) of the untreated wool fabrics are 14 s and 13 s, respectively. After the flame reaches the fixture, it can only reach the V-2 grade of UL-94 in the vertical burning test. As compared with untreated wool fabrics, with the increased WG of the treated wool fabrics, it gradually becomes difficult to ignite, and the length of char residue after burning is also reduced. The burning rate of the wool fabrics treated with 27.4% WG was slower, and a large amount of foam char was produced. Meanwhile, the t_1 and t_2 were all reduced to 0, and the char length was 3.1 cm and had self-extinguishment. It reached the V-0 grade of UL-94 the vertical burning test. Which is responsible for the phosphorus being able to strengthen the action mechanism of the system in the condensed phase, so as to accelerate the carbonization of wool fabric. PO · and other active factors

can be released in the gas phase, which can be thermally decomposed into pyrophosphoric acid and polyphosphate to catalyze the formation of carbon and protect the matrix from combustion. Nitrogen can make the system release more inert gases, such as NH_3, N_2 and other non-combustible gases [30], dilute the concentration of O_2 and other combustible gases in the combustion zone, bubble the carbon layer, produce expansion effect, and have a flame retardant effect in the condensed phase and gas phase at the same time.

As depicted in Fig. 7, the SEM of char residue for the untreated and treated wool with 27.4% WG under different magnification is presented. The fiber structure of char residue for the untreated wool was obviously damaged, and produced a flattened residue with a fragile character due to its relatively poor char forming ability. On the contrary, the fiber structure of treated wool fabrics char residue retained their partial textile structures after combustion, which is an evidence of enhanced char forming ability, indicating that ANPP can effectively protect the structure of the fabric after burning. When the intumescent ANPP is heated, the carbonization agent (carbon source) is dehydrated into carbon under the action of carbonization catalyst (acid source), and the carbide forms a fluffy carbon layer with porous closed structure under the action of the gas decomposed by the expansion agent. Once formed, it is incombustible and can weaken the heat conduction between the polymer and the heat source and prevent the diffusion of combustible gas. Once the combustion does not get enough fuel and oxygen, the burned polymer will extinguish itself, so as to achieve flame retardant effect. In addition, there are fine particles on the fiber surface, which is because the excessive ANPP molecules fail to graft with the active groups in the wool fiber molecules, but the fine particles are attached to the fiber surface in the form of coating at high temperature. This suggests ANPP can unquestionably act as an effective charring and ANPP agent in the condensed phase.

7. CONE Analysis

The combustion performance of the samples in real fire on 50 kW/m^2 heat flux (because the treated wool with 27.4% WG does not catch fire at 35 kW/m^2) was evaluated by CONE. The curves of HRR, THR, smoke generation rate (SPR) and total smoke generation rate (TSP) for untreated and treated wool before and after 50 LCs are displayed in Fig. 8(a) and (b), and various combustion parameters are listed in Table 4. The HRR and THR of treated wool fabrics before and after 50 LCs were obviously lower than those of untreated wool fabrics. The PHRR of untreated wool was up to 251.7 kW/m^2. In contrast, the treated wool fabrics were greatly reduced to 82.2 and 36.3 kW/m^2, respectively. The THR obviously

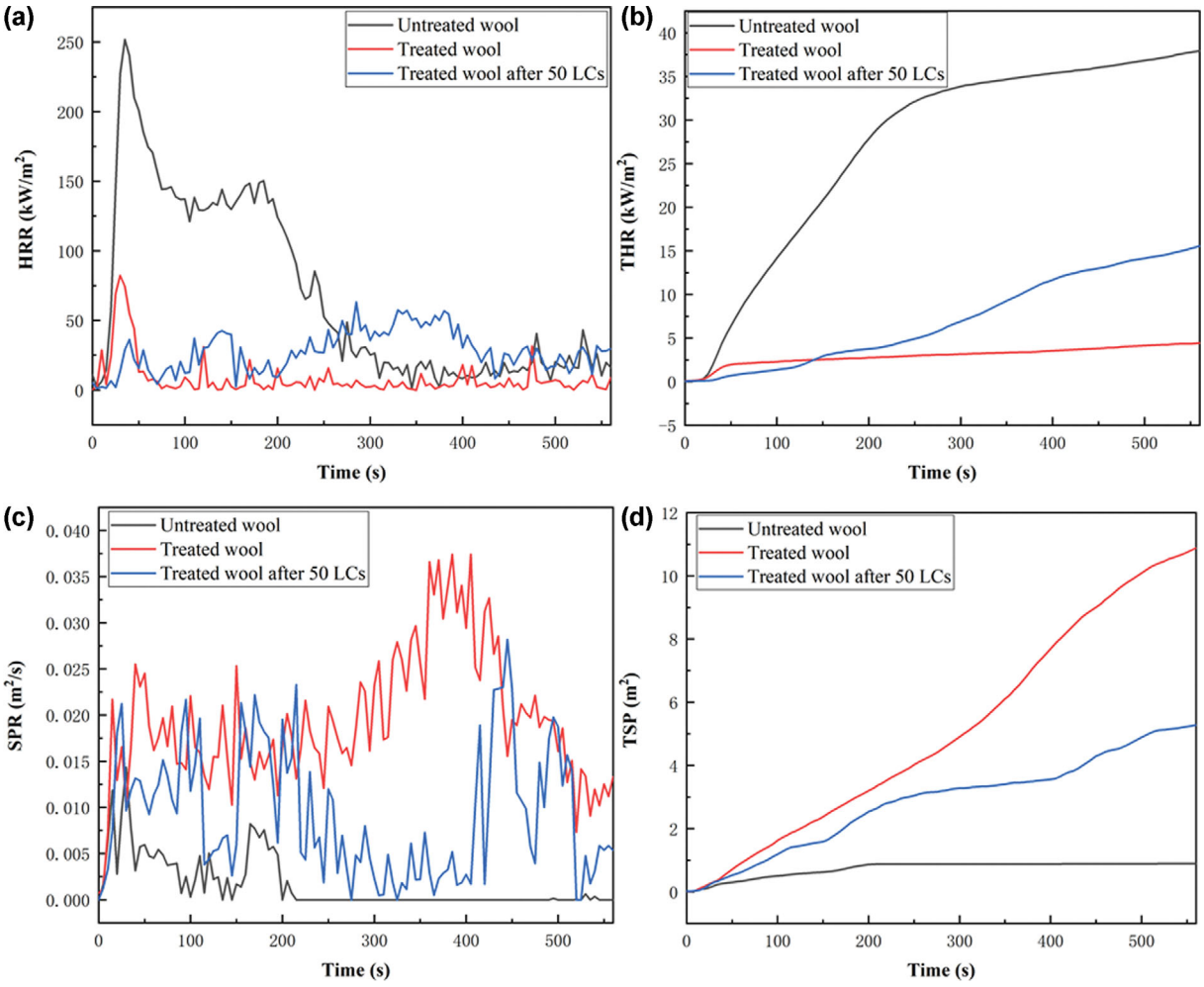

Fig. 8. (a) HRR, (b) THR, (c) SPR, and (d) TSP curves of the wool fabrics before and after ANPP finishing under 50 kW/m^2.

Table 4. Detailed data of the CONE tests for the wool fabrics before and after ANPP finishing

Heat flux	50 kW/m^2		
Sample	Untreated wool	Treated wool	Treated wool after 50 LCs
TTI (s)	15±1	33±2	16±1
PHRR (kW/m^2)	251.7±0.6	82.2±0.8	36.3±0.4
T_{PHRR} (s)	35.0±0.6	30.0±0.8	40.0±0.9
THR (MJ/m^2)	37.9±0.03	4.4±0.01	15.6±0.06
FRI	-	58.03	17.97
FIGRA (kW/m^{2}s)	7.17	2.27	0.90
TSP (m^2)	0.89±0.05	10.88±0.08	5.28±0.04
SEA (m^2/kg)	41.41	808.90	387.53
Av-EHC (MJ/kg)	20.88	3.67	12.44
av-COY (kg/kg)	0.037	0.097	0.055
av-CO_2Y (kg/kg)	2.73	1.27	1.30
Residue (%)	21.3±0.4	42.6±0.2	33.5±0.3

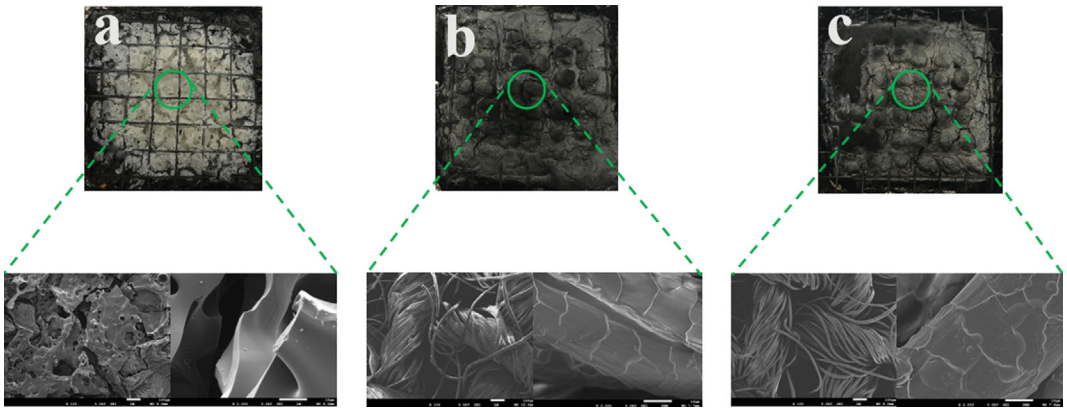

Fig. 9. CONE test results char residue of Digital and SEM micrographs for the a untreated, b treated wool fabrics, and c after 50 LCs.

declined to 4.4 and 15.6 MJ/m^2 from 37.9 MJ/m^2 than that of the untreated wool fabrics. In addition, the Flame Retardancy Index (FRI) of the samples was counted according to Eq. (2), and the FRI of treated wool fabrics was 58.03 (labeled "Excellent") and after 50 LCs was 17.97 (labeled "Excellent"), respectively [31]. Also, the fire growth rate index (FIGRA=PHRR/T_{PHRR}) of the untreated wool was as high as 7.17 kW/m^{2}s, while that of the treated wool before and after 50 LCs was clearly reduced to 2.27 and 0.90 kW/m^{2}s, respectively. It greatly increased the chances of people fleeing a fire.

The SPR and TSP for wool fabrics are depicted in Fig. 8(c) and (d). SPR and TSR are important parameters for evaluating the smoke emission of materials during combustion. SPR refers to the amount of smoke produced by the material per unit time. Smoke generation rate can be used to measure the shading of smoke and is an important index to evaluate the degree of fire hazard. TSP represents the degree of smoke emission of materials during combustion, so as to evaluate the smoke emission behavior of materials during combustion. The specific extinction area (SEA) listed in Table 4 presents a similar trend. The TSP of treated wool fabrics before and after 50 LCs increased to 10.88 and 5.28 m^2 from 0.89 m^2 than that of the untreated wool fabrics. This phenomenon may be ascribed to the formation of a compact char layer. Additionally, the average CO yield (av-COY) of treated wool increased and corresponding average CO_2 yield (av-CO_2Y) declined; this is caused by insufficient combustion of treated wool fabric. Meanwhile, the decrease in the average of the effective heat of combustion (av-EHC) suggested that the treated wool did not burn completely owning to the lower level of burning of combustion volatile gas [32]. It can be seen that the char residue of treated wool fabrics before and after 50 LCs was enhanced from 21.3 to 42.6 and 33.5%, respectively. It was speculated that the phosphorus-nitrogen compound facilitated the char formation during burning area. When the wool fabrics were ignited, the treated wool immediately formed a dense expansive protective carbon layer on the surface to effectively prevent the propagation of combustible gas and heat, which is the reason for the significant reduction of HRR and THR [33,34].

The digital and SEM of the untreated and treated wool with 27.4% WG before and after 50 LCs were obtained from the CONE test. As depicted Fig. 9(a), the original fiber structure of wool fabric was seriously damaged after the CONE test, and showed fragile thin carbon due to complete combustion and insufficient carbon formation. In contrast, the morphology and structure of treated wool char residue are more compact, and the structure was still retained. It can be inferred that ANPP finishing can reduce the

Table 5. Summary of flame retardant wool fabrics reported in recent years

Flame retardant	WG (%)	LOI (%)		Vertical burning char length (mm)		CONE		Reference
		0 LCs	50 LCs	0 LCs	50 LCs	PHRR (kW/m^2)	THR (MJ/m^2)	
FR-W	32.2	36.5	29.6	-	-	26.7	4.8	[35]
WS20	16.65	35.8	-	33	-	38.15	3.68	[14]
PEC	19.8	33.3	-	116	-	81.0	8.1	[36]
DBD	15.1	34.7	-	149	-	26.57	2.82	[37]
ANPP	27.4	37.8	30.5	31	71	82.2	4.4	This work

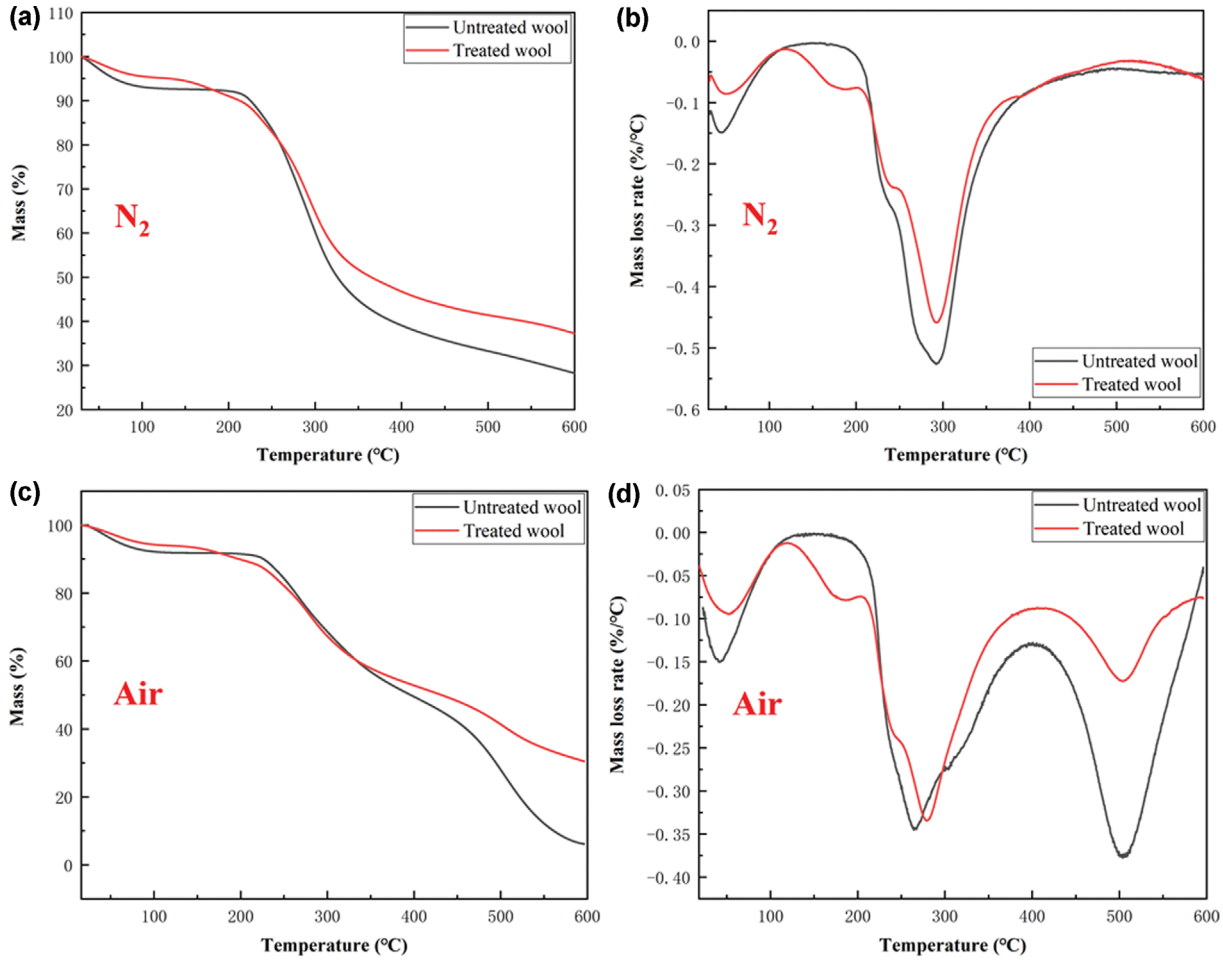

Fig. 10. TG and DTG curves of the (a), (b) untreated and treated wool fabrics under nitrogen and (c), (d) air atmospheres.

degree of combustion and thermal cracking of wool and improve the flame retardant properties of wool. The flame-retardant mechanism of ANPP can be summarized as follows. When exposed to flame or heat flow, ANPP first decomposes and releases phosphoric acid, which can catalyze the formation of thermally stable coke and phosphorus rich expansion structure. These changes block the transfer of heat and O_2 between gas and condensed phase. So as to prevent the further combustion of the underlying wool fiber, so as to improve the flame retardancy and thermal stability of the wool fabrics. Therefore, ANPP can improve the flame retardancy of wool through the action of condensed phase. To further determine the flame retardancy and durability of ANPP, Table 5 lists examples of different flame retardants applied to wool fabrics in recent years; it can be seen from Table 5 that ANPP treated wool fabric has good flame retardancy and durability.

$$FRI = \frac{\left[THR*\left(\frac{PHRR}{TTI}\right)\right]_{Neatpolymer}}{\left[THR*\left(\frac{PHRR}{TTI}\right)\right]_{Composite}} \quad (2)$$

FRI was calculated by Eq. (2).

8. TG Test

The thermal and thermal-oxidative stability of the untreated and treated wool with 27.4% WG were analyzed by TGA under N_2 and air atmospheres, respectively. The relevant curves of TG and DTG are displayed in Fig. 10 and the detailed data are listed in Table 6.

Table 6. Crucial data of the TG tests for the wool fabrics before and after ANPP finishing in nitrogen and air atmospheres

Sample	N_2 atmosphere				Air atmosphere					
	T_{10} (°C)	T_{max} (°C)	R_{max} (%/°C)	Residue at 600 °C (%)	T_{10} (°C)	T_{max1} (°C)	R_{max1} (%/°C)	T_{max2} (°C)	R_{max2} (%/°C)	Residue at 600 °C (%)
Untreated wool	225.32	292.33	0.53	28.25	226.31	264.26	0.35	504.26	0.38	6.14
Treated wool	212.88	291.43	0.46	37.24	197.94	278.90	0.33	503.81	0.17	30.47

T_{10} is the temperature where the untreated and treated wool fabrics lost 10%. T_{max} is the maximum-rate degradation temperature, and R_{max} is the maximum decomposition rate.

From Fig. 10(a) and (b), the pyrolysis process of wool fabrics in N_2 can be divided into two stages. The first stage is observed between 30 and 150 °C, which was attributed to the removal of physically bound moisture from wool fabrics. The second stage occurs from 190 to 450 °C, assigned to the pyrolysis reaction of wool fabrics. During this stage, the hydrogen bond peptides have helical structure and undergo solid-liquid phase changes in the ordered region of wool fabrics. Additionally, disulfide bonds break and release a large number of volatiles, including H_2S and SO_2. As presented in Table 6, the treated wool fabrics present lower T_{10}, T_{max}, and R_{max} values than the untreated wool fabrics; it is proved that the thermal degradation process is advanced. It was speculated that ANPP come into being phosphoric acid and polyphosphoric acid during thermal degradation stage; the earlier thermal degradation process of ANPP also accelerated the initial thermal degradation of the wool fabrics, which was expected to catalyze the thermal degradation of the wool fabrics, thus favoring the char residue formed and improving the thermal stability. Particularly, the ANPP can effectively increase the char residue mass to 37.24 from 28.25% of the untreated wool fabrics. In general, the pyrolysis reaction of wool fiber is mainly carried out in two possible directions: (1) wool fibers dehydrated and carbonized to generate H_2O, CO_2, and char residue; (2) wool fibers depolymerized to generate nonvolatile liquid L-glucose, which was further cracked to produce low molecular weight lysates and form secondary coke. In this work, ANPP decomposes into phosphoric acid and polymetaphosphoric acid during heating, which promotes the dehydration process of wool fiber, dehydrates wool fiber into carbon in advance and reduces the content of combustible gas released [38]. As described in direction (1), a dense char barrier is formed on the surface of wool fiber, which effectively inhibits the further degradation of wool fiber [39-41].

From Fig. 10(c) and (d), the TG curves under air atmosphere have changed; for the untreated wool fabrics, the first two stages are similar in N_2 atmosphere, and the third stage is mainly char oxidation. In this process, the char residue and the hydrocarbon are further oxidized to CO and CO_2, so the weight loss rate is higher. For the treated wool fabrics, there are only two thermal decomposition stages, during which no further coking and oxidation process is involved [42-44]. Only 6.14% of char residue for the untreated wool is left at 600 °C and the treated wool has a char residue of 30.47% under air atmosphere, which is lower than that of the char residue under N_2 atmosphere (37.24%). And the TG curve did not see a stable state, so the char residue at high temperature is unstable, which proves the time extension of the treated wool thermal

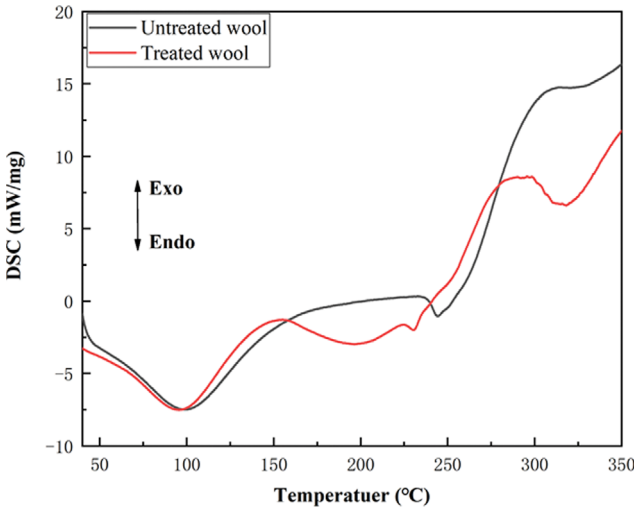

Fig. 11. DSC curves of the wool fabrics before and after ANPP finishing.

decomposition process. Under air conditions, the higher carbon residue indicates that the char residue of flame retardant wool has higher oxidation resistance and thermal insulation properties.

9. DSC Tests

The thermal properties of the untreated wool and wool treated with 27.4% WG were evaluated by DSC under N_2 atmosphere, and the DSC curves are depicted in Fig. 11. Apparently, wool fabrics show a wide endothermic characteristic peak located at 100 °C. The reason can be explained that the bound water inside the wool fabric was consumed and absorbed a great quantity of heat [45]. Treated wool fabrics have an exothermic peak around 290 °C. During this period, the decomposition of phosphorus containing compounds can release active phosphorus containing groups (phosphoric acid, polymetaphosphoric acid, etc.) [46], and an expanded protective carbon layer is formed on the surface of polymer materials through chemical reactions (hydrolysis, dehydration, chain breaking or chain breaking, etc.) [47]. The existence of these protective carbon layers isolates the fire source from the polymer matrix, slows the degradation rate of the polymer, and finally reduces the combustion time.

10. Flame-retardant Mechanism Analysis

The flame retardancy of polymer materials is closely related to the graphitized carbon content of char residue. Higher graphitization carbon degree is conducive to better thermal resistance and greater protection effect [48,49]. Raman spectroscopy has been widely used to study the graphitization carbon degree of chars. Further, to better discover the flame-retardant mechanism of ANPP, the char

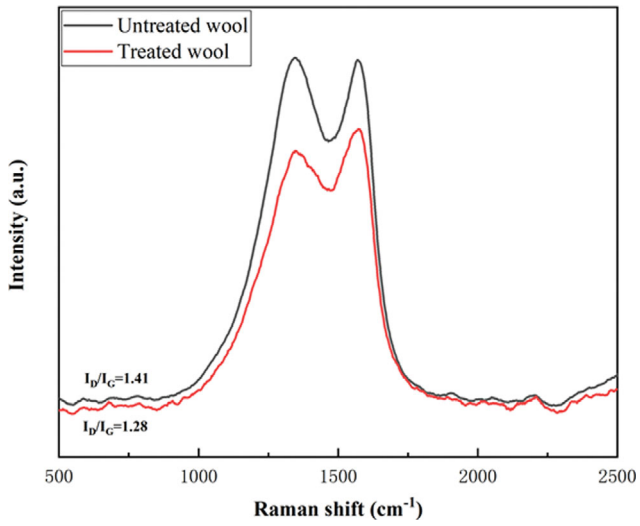

Fig. 12. Raman spectra for the wool fabrics char residue before and after ANPP finishings after CONE test.

residue of the untreated wool and wool treated with 27.4% WG after CONE test was observed by Raman spectra. As shown Fig. 12, there two absorption bands appeared at the 1,349 and 1,571 cm^{-1}, respectively, which represented the D and G bands, and the intensity of the D band represents the disorder and structural integrity of carbon materials, such as edge carbon, defective carbon. The G band stands for the stretching vibration in the SP^2 hybrid plane of C atom, and its strength represents the order and integrity of carbon materials [50]. Generally, the integral strength ratio (I_D/I_G) could be applied to estimate the graphitization degree of residual carbon; a lower I_D/I_G value indicates that the graphitization degree of residual carbon is higher. Therefore, the graphitized carbon layer formed in the pyrolysis process plays a vital role in control of mass and heat transfer and a more significant protective effect on wool fabric [51-53]. As exhibited in Fig. 12, the I_D/I_G of the treated wool fabrics dropped from 1.41 to 1.28, demonstrating the ANPP can accelerate the shape of a graphitized char layer

Table 7. Element contents of the wool fabrics for the char residue before and after ANPP finishing after CONE test

Sample	C (%)	O (%)	N (%)	P (%)
Untreated wool	45.28	39.06	8.66	-
Treated wool	53.95	21.38	11.34	13.33

in the course of burning [54]; this obviously improves the flame retardancy of wool.

The XPS results of the untreated wool and wool treated with 27.4% WG after CONE test are displayed as Fig. 13; the relevant data are listed in Table 7. Fig. 13(a) shows the untreated wool fabrics of O 1s, N 1s, and C 1s, located at 531.1, 399.2 and 284.0 eV, respectively. It was noticed that the treated wool fabrics had a characteristic peak of P2p at 131.2 eV, reflecting the appearance of phosphorus components. From Table 7, for the treated wool fabrics, C increased to 53.95 from 45.28% and O decreased to 21.38% from 39.06%. It is speculated that polyphosphate and metaphosphoric acid derivatives formed by phosphorus-containing compounds were catalyzed the formation of char residue, while ANPP can promote carbonization, and a large amount of CO_2 and H_2O are generated at high temperature, thereby an increase in the C content and decrease in the O content It also indicates that ANPP plays a typical flame retardant effect in the condensed phase. In addition, P element was detected in the treated wool fabrics, which proved that ANPP existed in the interior of the treated wool fabrics. More interestingly, compared with the treated wool fabrics before burning, it can be clearly observed that the N content of the treated wool fabrics after burning decreases from 20.14% to 11.34%, and the P content increases from 9.46% to 13.33%. Which should be attributed to ANPP releasing a large amount of noncombustible gases such as NH_3 and N_2 at high temperature, diluting the concentration of O_2, slowing the combustion speed until the flame goes out, resulting in the N content decreased, reflecting that ANPP has a typical vapor phase flame-retardant mechanism.

Further utilized to study the chemical structure of the untreated and treated wool fabrics, we characterized the P 2p spectra of the

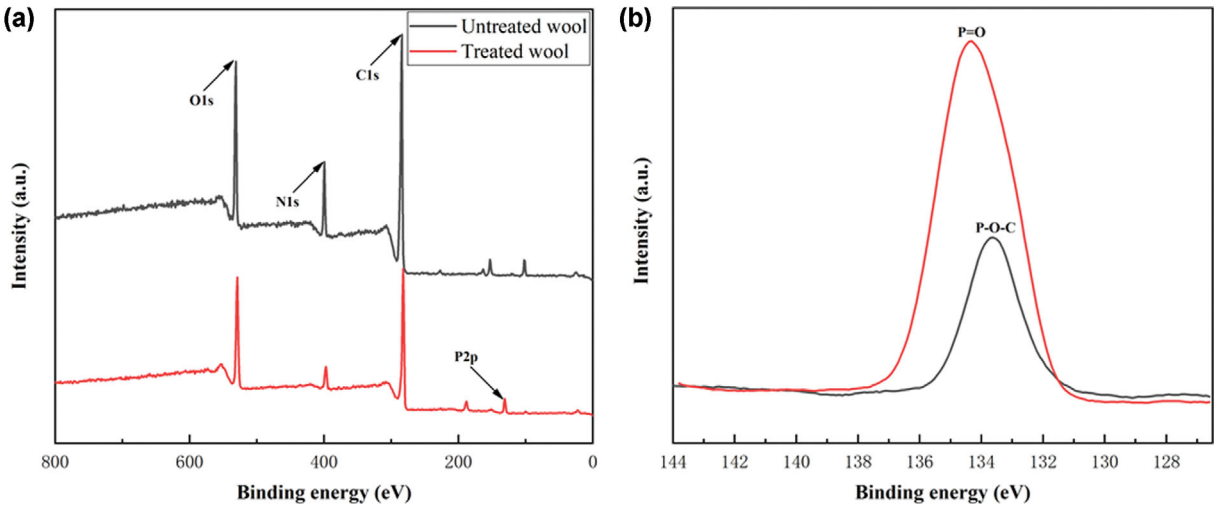

Fig. 13. (a) XPS curves of the untreated and treated wool fabrics and (b) P 2p of the treated wool fabrics for the char residue after CONE test.

untreated and treated wool fabrics for the char residue after the CONE test. As shown in Fig. 13(b), the P 2p spectra of treated wool fabrics have two peaks, at 133.7 and 134.2 eV, which correspond to P-O-C bond and P=O bond, respectively [55]. The presence of P-O-C indicates the phosphorylation of wool fibers during the burning, which confirms that phosphorus-nitrogen compounds formed, reflecting that the phosphorus-nitrogen char layer protected the underlying wool fibers, thereby inhibiting the further combustion and thermal degradation.

CONCLUSION

We creatively designed a new phosphorus-nitrogen flame retardant and successfully applied it to wool fabrics. Flame retardant treatment significantly enhanced its flame retardance. XRD analysis showed that the crystal structure for the treated wool fabrics was almost unchanged, the LOI of the treated wool fabrics achieved 37.8% with a WG of 27.4%. Wool fabrics treated with a WG of more than 27.4% can achieve lasting flame retardancy. Furthermore, the results of the CONE test showed that the PHRR and THR values obviously declined by 67.3% and 88.4% of the treated wool fabrics. The char residue at high temperatures demonstrated that the ANPP was beneficial for forming a dense phosphorus-nitrogen char layer that can effectively reduce the diffusion of heat and combustible gases, playing flame retardancy in the condensed phase. Additionally, the physical properties of wool fabrics basically remained. In terms of economic cost, the raw materials used in this study (such as DEA, phosphorous acid, phosphoric acid, and urea, etc.) are easy to obtain and relatively cheap, and formaldehyde is not released in the whole process. Combined with the advantages of high efficiency, durability, and eco-friendliness, this ANPP presents huge potential applications in the industrial and product fields.

ACKNOWLEDGEMENTS

We greatly appreciate the financial support from the projects of NSFC (No. 22106051) and Jilin Science and Technology Bureau (No. 20190104190, No.20190104189).

DECLARATION OF COMPETING INTEREST

The authors declare that they have no known competing financial interests or personal relationships that could have appeared to influence the work reported in this paper.

REFERENCES

1. J. M. Cardamone, *Handbook of fire resistant textiles*, Woodhead Publishing Limited, Cambridge, 245 (2013).
2. P. Zhu and G. Sun, *J. Appl. Polym. Sci.*, **93**, 1037 (2004).
3. Q. H. Zhang, W. Zhang, J. Y. Huang, Y. K. Lai, T. L. Xing, G. Q. Chen, W. R. Jin, H. Z. Liu and B. Sun, *Mater. Des.*, **85**, 796 (2015).
4. R. V. Khose, D. A. Pethsangave, P. H. Wadekar, A. K. Ray and S. Some, *Carbon*, **139**, 205 (2018).
5. L. S. Birnbaum and D. F. Staskal, *Environ. Health Perspect*, **112**, 9 (2004).
6. J. F. Li, W. Jiang and M. L. Liu, *Cellulose*, **29**, 4725 (2022).
7. K. C. Patankar, S. Maiti, G. P. Singh, M. Shahid, S. More and R. V. Adivarekar, *Clean. Eng. Technol.*, **5**, 100319 (2021).
8. L. Benisek and W. A. Phillips, *J. Fire Sci.*, **1**, 418 (1983).
9. S. Basak, K. K. Samanta, S. K. Chattopadhyaya, P. Pandit and S. Maiti, *Color. Technol.*, **132**, 135 (2016).
10. P. J. Davies, A. R. Horrocks and M. Miraftab, *Polym. Int.*, **49**, 1125 (2000).
11. A. R. Horrocks and S. Zhang, *Text. Res. J.*, **74**, 433 (2004).
12. X. W. Cheng, J. P. Guan and X. H. Yang, *J. Clean. Prod.*, **223**, 342 (2019).
13. X. W. Cheng, J. P. Guan and X. H. Yang, *Thermochim. Acta*, **665**, 28 (2018).
14. P. Mathur, J. N. Sheikh and K. Sen, *Polym. Degrad. Stabil.*, **174**, 109101 (2020).
15. Z. Zhou, W. R. Bao, Y. B. Di and J. M. Dai, *Fiber Polym.*, **16**, 560 (2015).
16. J. F. Li and W. Jiang, *Ind. Crop Prod.*, **174**, 114205 (2021).
17. D. A. Pethsangave, R. V. Khose, P. H. Wadekar and S. Some, *ACS Appl. Mater. Interfaces*, **9**, 35319 (2017).
18. D. A. Pethsangave, R. V. Khose, P. H. Wadekar and S. Some, *ACS Sustain. Chem. Eng.*, **7**, 11745 (2019).
19. F. Razmjooei, K. P. Singh, E. J. Bae and J. S. Yu, *J. Mater. Chem.*, **3**, 11031 (2015).
20. X. Y. Guo, Y. Miao, P. P. Ye, Y. Wen and H. F. Yang, *Mater. Res. Express*, **1**, 025403 (2014).
21. W. W. Gao, G. X. Zhang and F. X. Zhang, *Cellulose*, **22**, 2787 (2015).
22. H. L. Liu and W. D. Yu, *J. Appl. Polym. Sci.*, **103**, 1 (2007).
23. A. A. Farag, *Spectrochim. Acta Mol. Biomol. Spectrosc.*, **65**, 667 (2006).
24. Y. L. Jia, Y. W. Hu, D. D. Zheng, G. X. Zhang, F. X. Zhang and Y. J. Liang, *Cellulose*, **24**, 1159 (2016).
25. D. D. Zheng, J. F. Zhou, Y. Wang, F. X. Zhang and G. X. Zhang, *Cellulose*, **25**, 787 (2017).
26. O. Kareb, A. Gomaa, C. P. Champagne, J. Jean and M. Aider, *Food Chem.*, **221**, 590 (2017).
27. M. S. Khalil-Abad, M. E. Yazdanshenas and M. R. Nateghi, *Cellulose*, **16**, 1147 (2009).
28. S. C. Chang, B. Condon, E. Graves, M. Uchimiya, C. Fortier, M. Easson and P. Wakelyn, *Fibers Polym.*, **12**, 334 (2011).
29. X. H. Li, H. Y. Chen, W. T. Wang, Y. Q. Liu and P. H. Zhao, *Polym. Degrad. Stabil.*, **120**, 193 (2015).
30. A. Nallathambi and R. G. D. Venkateshwarapuram, *Carbohydr. Polym.*, **152**, 1 (2016).
31. H. Vahabi, B. K. Kandola and M. R. Saeb, *Polymers*, **11**, 407 (2019).
32. M. S. Liu, S. Huang, G. X. Zhang and F. X. Zhang, *Cellulose*, **26**, 7553 (2019).
33. P. Zhao, W. H. Rao, H. Q. Luo, L. Wang, Y. L. Liu and C. B. Yu, *Mater. Des.*, **193**, 108838 (2020).
34. W. T. He, P. G. Song, B. Yu, Z. P. Fang and H. Wang, *Prog. Mater. Sci.*, **114**, 100687 (2020).
35. Y. S. Liu, Y. B. Guo, Y. L. Ren, Y. Wang, X. Guo and X. H. Liu, *Polym. Degrad. Stabil.*, **179**, 109286 (2020).
36. X. W. Cheng, R. C. Tang, F. Yao and X. H. Yang, *Prog. Org. Coat.*, **132**, 336 (2019).

37. W. Jiang, J. F. Li, Z. Y. Li, X. Y. Zhang, F. L. Jin and S. J. Park, *Korean J. Chem. Eng.*, **38**, 872 (2021).
38. E. Kaynak, M. E. Ureyen and A. S. Koparal, *Mater. Today: Proceedings*, **31**, S258 (2020).
39. X. W. Cheng, J. P. Guan, G. Q. Chen, X. H. Yang and R. C. Tang, *Polymers*, **8**, 122 (2016).
40. R. Zhang, X. F. Xiao, Q. L. Tai, H. Huang and Y. Hu, *Polym. Eng. Sci.*, **52**, 2620 (2012).
41. F. Carosio, J. Alongi and G. Malucelli, *Polym. Degrad. Stabil.*, **98**, 1626 (2013).
42. M. Forouharshad, M. Montazer, M. B. Moghadam and O. Saligheh, *Thermochim. Acta*, **520**, 134 (2011).
43. C. M. Tian, Z. Li and H. Z. Guo, *J. Fire Sci.*, **21**, 155 (2003).
44. A. R. Horrocks and P. J. Davies, *Fire Mater.*, **24**, 151 (2000).
45. C. Colleoni, I. Donelli, G. Freddi, E. Guido, V. Migani and G. Rosace, *Surf. Coating. Technol.*, **235**, 192 (2013).
46. Y. L. Ren, Y. T. Gu, Q. Zeng and Y. Zhang, *Eur. Polym. J.*, **94**, 1 (2017).
47. A. Taherkhani and M. Hasanzadeh, *Mater. Chem. Phys.*, **219**, 425 (2018).
48. X. Zhou, S. L. Qiu, W. Cai, L. X. Liu, Y. B. Hou, W. Wang, L. Song, X. Wang and Y. Hu, *Chem. Eng. J.*, **369**, 451 (2019).
49. W. W. Guo, B. Yu, Y. Yuan, L. Song and Y. Hu, *Compos. Part B: Eng.*, **123**, 154 (2017).
50. L. Chen and Y. Z. Wang, *Polym. Adv. Technol.*, **21**, 1 (2010).
51. J. L. Wang, D. C. Zhang, Y. Zhang, W. Cai, C. X. Yao, Y. Hu and W. Z. Hu, *J. Hazard. Mater.*, **362**, 482 (2019).
52. X. Zhou, S. L. Qiu, W. Y. Xing, C. S. R. Gangireddy, Z. Gui and Y. Hu, *ACS Appl. Mater. Interfaces*, **9**, 29147 (2017).
53. Y. Q. Shi, B. Yu, Y. Y. Zheng, J. Yang, Z. P. Duan and Y. Hu, *J. Colloid Interface Sci.*, **521**, 160 (2018).
54. L. J. Duan, H. Y. Yang, L. Song, Y. B. Hou, W. Wang, Z. Gui and Y. Hu, *Polym. Degrad. Stabil.*, **134**, 179 (2016).
55. J. Gorham, J. Torres, G. Wolfe, A. d'Agostino and D. H. Fairbrother, *J. Phys. Chem. B*, **109**, 20379 (2005).